OPEN ACCESS

*International*
*Journal*
*Of Modern Engineering Research (IJMER)*

# Computational Analysis of Natural Convection in Spherical Annulus Using FEV

Md Shoaib Khan[1], Manish Bhaskar[2], Sankalp Verma[3]

***Abstract*:** *HEAT transfer by natural convection from a body to its finite enclosure is of importance in nuclear reactor technology, electronic instrumentation packaging, aircraft cabin design, the analysis of fluid suspension gyrocompasses, and numerous other practical situations. The steady natural convection heat transfer of fluids between two concentric isothermal spheres is investigated computationally with the help of FEV in ANSYS 14.5. The inner wall is subjected to a higher temperature and outer is at room temperature. The steady behavior of the flow field and its subsequent effect on the temperature distribution for different Rayleigh numbers and radius ratios are analyzed.*

*Bossious boundary condition is taken for natural convection and which is solved in fluent module. Steady solutions of the entire flow field is obtained for Rayleigh number (5x101<Ra<105), various Prandlt number and radius ratio (l.5<rr<3). The result shows that the Rayleigh number and radius ratio have a profound influence on the temperature and flow fields and Prandlt number has very negligible effect. The results of average Nusselt numbers are also compared with those of previous numerical investigations. Excellent agreement is obtained.*

***Key Words:*** *Convection, Nusselt Number, Ansys*.

## I. INTRODUCTION

HEAT transfer by natural convection from a body to its finite enclosure is of importance in nuclear reactor technology, electronic instrumentation packaging, aircraft cabin design, the analysis of fluid suspension gyrocompasses, and numerous other practical situations. Accurate prediction of such heat-transfer rates, which can now only be roughly approximated, is required in many engineering design problems. Since natural convection flow fields are buoyancy driven due to thermal effects, the thermal fields and hydrodynamic fields are very closely coupled, and knowledge of the flow field is essential to the complete understanding of the heat-transfer phenomena. Also, the unusual stability conditions associated with this problem are of fundamental interest in the fields of heat transfer and fluid mechanics.

In 1968 analytical investigation of natural convection in annuli between two isothermal concentric spheres, the inner surface being hotter, was initiated by Mack and Hardee, the solution for steady axisymmetric natural convection between isothermal concentric spheres is obtained.

In 1973 yin and powe conduct experimental investigation to describe concerning the natural convection flow patterns which occur in the annular space between two concentric isothermal spheres, the inner one being hotter. The several types of flow patterns observed are correlated with previously published temperature profiles and are categorized in terms of steady and unsteady regimes.

In 1976 Douglass perform steady forced convection of a viscous fluid contained between two concentric spheres which are maintained at different temperatures and rotate about a common axis with different angular velocities is considered. The resulting flow pattern, temperature distribution, and heat-transfer characteristics are presented for the various cases considered.

Ralph and scanlan 1977 results of a flow visualization study of natural convection in liquids contained between a heated sphere and its cooled cubical enclosure are reported Interference between up-flow and down-flow layers was noted for the smallest dimension ratio, and this created a rather unique flow pattern.

Ramadhyani et al 1984 presents numerical finite difference solutions of combined natural and forced convective heat transfer in spherical annuli. The result the buoyancy effects can have a very significant impact on the heat transfer and fluid flow, particularly at low Reynolds numbers.

Sanjay and sengupta 1988 examine the results of a numerical investigation of the natural convection process between isothermal vertically eccentric spheres with hotter inner core, and fount that Negative eccentricities have been found to enhance convection while positive eccentricities have the reverse effect.

Results also show that heat transfer actually increases slightly for very high positive eccentricities where conduction plays an important role.

Garg in 1992 give a finite-difference solution for steady natural convective flow in a concentric spherical annulus with isothermal walls has been obtained. The stream function-vorticity formulation of the equations of motion for the unsteady axisymmetric flow is used; interest lying in the final steady solution.

Chiu and Shich 1999 perform A numerical analysis determine the heat transfer of micropolar fluids by natural convection between concentric spheres with isothermal boundary conditions Results indicate that the heat transfer rate of a micropolar fluid is smaller than that of a Newtonian fluid, and the main controlling parameter is the dimensionless vortex viscosity.

Vadim and rath 2002 The energy stability problem with respect to axisymmetric disturbances of the natural convection in the narrow gap between two spherical shells under the earth gravity is discussed. The results are compared with the results of the linear stability analysis for the same problem.

Wen and Yen 2008 the effects of micro-rotation and vortex viscosity in micropolar fluids have been investigated numerically to determine heat transfer by natural convection between concentric and vertically eccentric spheres with specified mixed boundary conditions.

InChen 2010 investigates the effects of eccentricity and geometric configuration with a Newtonian fluid, numerically to determine heat transfer by natural convection between the sphere and vertical cylinder with isothermal boundary conditions. Results of the parametric study conducted further reveal that the heat and flow fields are primarily dependent on the Rayleigh number, eccentricity and geometric configuration, for a Prandtl number of 0.7, with the Rayleigh number ranging from 103 to 106, the three eccentricities and two geometric configurations.

Alassar 2011 An exact solution of the problem of heat conduction in the annulus between eccentric isothermal spheres with internal heat generation is obtained. The solution is given in terms of the temperature distribution and local and average Nusselt numbers.

Sangita 2013 reports results of a numerical investigation of natural convection in a spherical porous annulus. The inner and outer surfaces are subjected to constant temperatures. The Brinkman extended Darcy flowmodel is considered in her study.

Hatami and ahangar 2014 present, temperature distribution equation for a fully wet semi-spherical porous fin. The driving forces for the heat and mass transfer are considered temperature and humidity ratio differences, respectively. , the effects of porosity, Darcy number, Rayleigh number, Lewis number, etc. on the fin efficiency are investigated.

## II. MATHEMATICAL MODELING

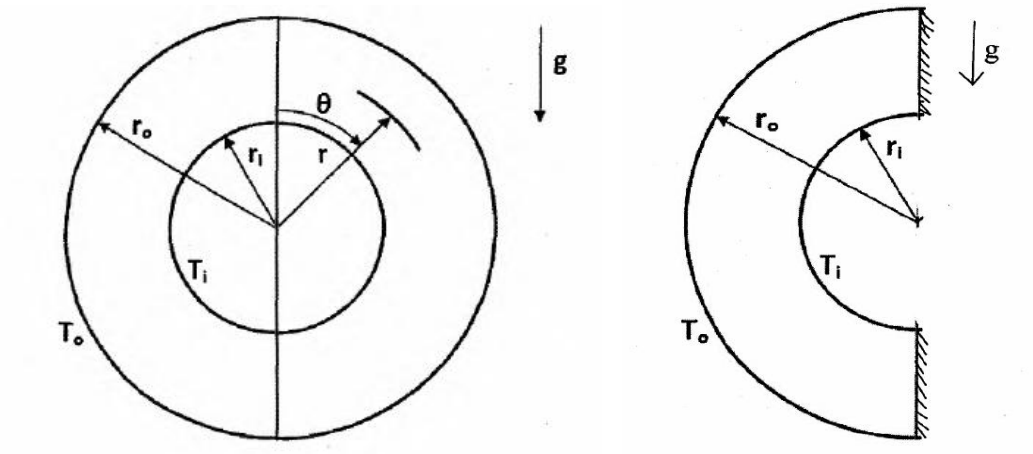


Figure 1 Physical model and coordinate system and Sectional view

figure 1 Here θ is the polar angle and varies from 0 to π The governing equations in polar coordinate are described in dimensional form specifying boundary conditions for velocity and temperature as below:

$$\frac{\partial}{\partial r}(r^2 u \sin\theta) + \frac{\partial}{\partial \theta}(r^2 v \sin\theta) = 0$$

$$u\frac{\partial u}{\partial r}+\frac{v\partial u}{r\partial\theta}-\frac{v^2}{r}=-\frac{1}{\rho_m}\frac{\partial p}{\partial r}$$
$$+\mu\left[\frac{1}{r^2}\frac{\partial}{\partial r}\left(r^2\frac{\partial u}{\partial r}\right)+\frac{1}{r^2\sin\theta}\frac{\partial}{\partial\theta}\left(\sin\theta\frac{\partial u}{\partial\theta}\right)-2\frac{u+\frac{\partial v}{\partial\theta}+v\cot\theta}{r^2}\right]-\frac{1}{\rho_m}\rho g\cos\theta \quad (2)$$

$$u\frac{\partial u}{\partial r}+\frac{v\partial u}{r\partial\theta}+\frac{uv}{r}=-\frac{1}{r\rho_m}\frac{\partial p}{\partial\theta}$$
$$+\mu\left[\frac{1}{r^2}\frac{\partial}{\partial r}\left(r^2\frac{\partial v}{\partial r}\right)+\frac{1}{r^2\sin\theta}\frac{\partial}{\partial\theta}\left(\sin\theta\frac{\partial v}{\partial\theta}\right)+\frac{2}{r^2}\frac{\partial u}{\partial\theta}-\frac{v}{r^2(\sin\theta)^2}\right]+\frac{1}{\rho_m}\rho g\sin\theta \quad (3)$$

$$u\frac{\partial T}{\partial r}+\frac{v}{r}\frac{\partial T}{\partial\theta}=\alpha\left(\frac{\partial^2 T}{\partial r^2}+\frac{1}{r^2}\frac{\partial^2 T}{\partial\theta^2}+\frac{2\partial T}{r\partial r}+\frac{\cot\theta}{r^2}\frac{\partial T}{\partial\theta}\right) \quad (4)$$

$$\rho=\rho_m\left[1-\beta(T-T_m)\right]$$

Boundary Condition

u=0, v=0, T=Ti at r=ri for 0≤θ
u=0, v=0, T=Ti at r=ro for 0≤θ≤π
u=0, v=0, dt/dθ=0 at θ=0 for ri≤r≤ ro
u=0, v=0, dt/dθ=0 at θ=π for ri≤r≤ ro

Non Dimensional Parameters

$$U=\frac{u}{a/d}\qquad T^*=\frac{T-T_c}{T_h-T_c}\qquad V==\frac{v}{a/d}\qquad P=\frac{\rho}{\mu\alpha/d^2}$$

$$R=r/d\qquad \bar{\rho}=\frac{\rho}{\rho_m}\qquad rr=\frac{r_o}{r_i}$$

Where rr (radius ratio)

$$rr=\frac{r_o}{r_i}$$

Pr (Prandlt Number)

$$\Pr=\frac{\mu}{\rho_m\alpha}=\frac{\vartheta}{\alpha}$$

Ra (Rayleigh Number)

$$Ra=\frac{g\beta\Delta Td^3}{\vartheta\alpha}$$

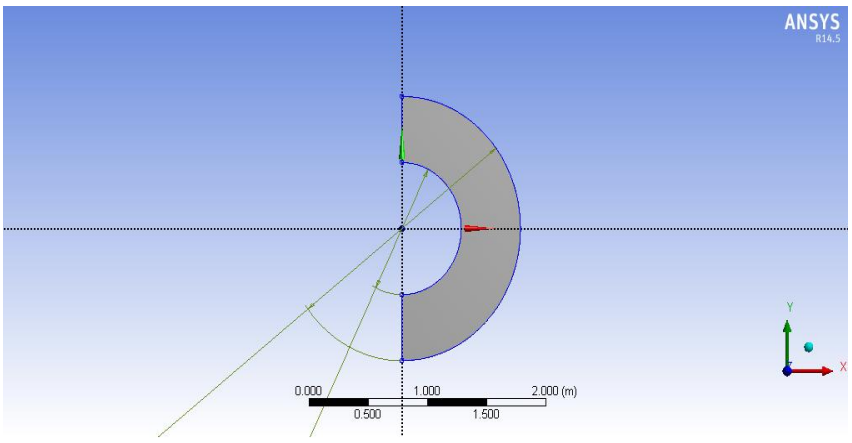


Figure 2 Model Geometry

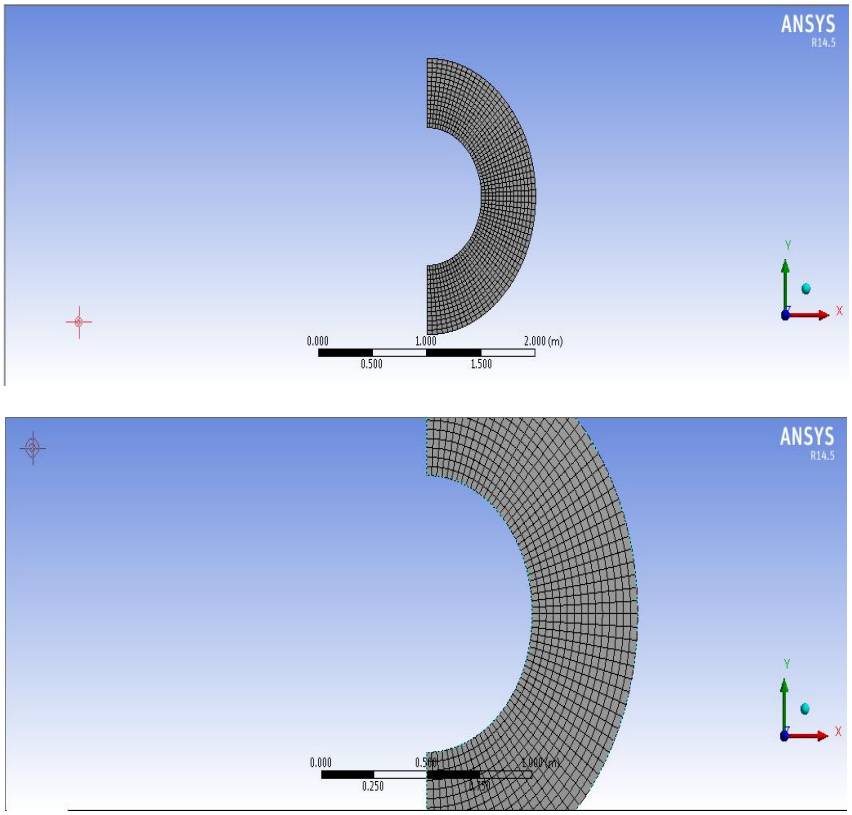


Figure 3 Mesh Model

## III. RESULTS

Natural convection between two concentric spheres, inner at constant higher temperature while the outer is at low temperature, filled with a fluid has been studied. Now the various results are obtained from the analysis using FEV scheme. The various effects of three non-dimensional parameters Rayleigh number (Ra), Prandlt number (Pr) .and radius ratio(rr) on flow field, temperature field and Nusselt number have been discussed in this chapter.

### *A. Grid Sensitivity Test*

Before studying the influence of the above three parameters on temperature field and flow field, the optimum values for some parameters used during calculation by FEV. Those parameters are optimum Grid size, acceleration factor (ω) and the optimum error tolerance limit (ε). First to the find the optimum grid size for numerical result the grid sensitivity test was conducted as shown in the table 1

**Table 1 Table Sensitivity test for rr = 2, Pr = 0.7 and Ra = $10^3$**

| Grid Size | $Nu_h$ | $Nu_c$ | Avg. Nusset Number |
|---|---|---|---|
| **20x20** | 1.99 | 1.99 | 1.99 |
| **30x30** | 1.97 | 1.97 | 1.97 |
| **40x40** | 1.96 | 1.96 | 1.96 |
| **50x50** | 1.96 | 1.96 | 1.96 |

Examining Table-1 shows that the smaller grid size 40x40 and 50x50 did not cause any significant changes in the magnitude of the average Nusselt number for the test cases a uniform grid size of 40x40 was chosen for calculation of all cases in the study.

On the basis of the grid size 40x40 the optimum value of acceleration factor was checked According to SAR scheme in literature the acceleration factor ω varies from 0 to 2.

Acceleration factor ω = 1 has been used for all the calculations having Ra < 3x $10^4$ while acceleration factor ω varies from 0.5 to 0.1 for higher Rayleigh due to the convergence criterion.

Table 2 shows the values of average Nusselt number for different error tolerance limit. Nusselt number value increases as the value of error tolerance limit increases and attains a steady state at ε=l$0^{-5}$. As

there has been marked very less changes in value between E value I0·5 and 10-6 in order to reduce the CPU time $10^{-5}$ has been used as optimum error tolerance limit.

**Table 2 Optimum error tolerance limit (ε) for Ra= 1000, Pr= 0.7 and rr= 2**

| Eps. Value | Nuh | Nuc | Avg.Nu |
|---|---|---|---|
| **0.0001** | 3.40459 | 3.52778 | 3.466185 |
| **0.00001** | .4281 | 3.45719 | 3.442645 |
| **0.000001** | 3.42988 | 3.45429 | 3.442085 |

All these values in table 2 were calculated for grid size 40x40, Ra= $10^5$, Pr=0.7, rr=2, $\omega_t = \omega_o = \omega_s$ =0.5. While for table -3 Ra= $10^4$, Pr= 0.7, rr=2, $\omega_t = \omega_o = \omega_s$ =1.

### *B. Validation of FEV scheme*

The values of different parameters like average Nusselt number and maximum stream function calculated using FEV and SAR scheme were being validated by earlier papers as seen in Table 3.

**Table 3 Comparison of Present work with reference papers at rr= 2, Pr= 0.7, Ra= $10^3$.**

| Reference | Avg. Nu | $\Psi_{max}$ |
|---|---|---|
| **H.W. Wu, Wen, C.Tsai [l0]** | 1.10 | 3.25 |
| **H.S. Chu, T.S.Lee [7]** | 1.09 | 3.21 |
| **Mack and Harde [1]** | 1.12 | 3.21 |
| **Present** | 1.1 | 3.23 |

Table.4 compares the results of present work with results from different paper, which shows the results are very accurate. The percentage of error varies between 0.90-1.181 for average Nusselt number and between 0.62- 7.38 for maximum stream function.

In Table 4 comparison of the present values has been done with the values as given in the paper of H.S.Chu and T.S.Lee[8] for different Rayleigh number. Before calculating the present data's for comparison, a relation is being developed between the expression for Rayleigh No used by Chu and Lee and the Present Rayleigh No. As it can be noticed from the table.5 that all our values are very much accurate. The relation being developed is

$$Ra_P = (rr-1)^3 \times Ra$$

Where, $Ra = \dfrac{g\beta\Delta T(r_i)^3}{\vartheta a}$, expression of Rayleigh number used by H.S.Chu and T.S.Lee

$Ra_p = \dfrac{g\beta\Delta T(r_o - r_i)^3}{\vartheta a}$ , expression of Rayleigh number used in present work

**Table-4 Comparison of FEV and SAR scheme result with H.S.Chu and T.S.Lee at Pr= 0.7 for different Ra value and radius ratio**

| rr | Ra | $Ra_p$ | Nusselt number (H.S.Chu and T.S.Lee) Ref. [10] | Average Nusselt number Present |
|---|---|---|---|---|
| 1.2 | $1x10^3$ | 8 | 1.00 | 1.00 |
| 1.2 | $1x10^4$ | $8x10^1$ | 1.00 | 1.00 |
| 1.2 | $1x10^5$ | $8x10^2$ | 1.01 | 1.01 |
| 1.5 | $1x10^2$ | $1.25x10^1$ | 1.00 | 1.00 |
| 1.5 | $1x10^3$ | $1.25x10^2$ | 1.00 | 1.00 |
| 1.5 | $1x10^4$ | $1.25x10^3$ | 1.07 | 1.07 |
| 1.5 | $1x10^5$ | $1.25x10^4$ | 1.92 | 1.95 |
| 1.5 | $1x10^6$ | $1.25x10^5$ | 3.71 | 3.47 |
| 2.0 | $1x10^2$ | $1x10^2$ | 1.00 | 1.00 |
| 2.0 | $1x10^3$ | $1x10^3$ | 1.10 | 1.10 |
| 2.0 | $1x10^4$ | $1x10^4$ | 1.97 | 1.96 |
| 2.0 | $1x10^5$ | $1x10^5$ | 3.49 | 3.43 |

### *C. Flow and Temperature fields*

Fig.4 and Fig.5 present streamline configurations, isotherms for radius ratio of 2.0, Prandlt number 0.7 at two different Rayleigh number $10^4$ and $10^5$. These results are designed to show the influence of the Rayleigh number on the flow field and isotherms. The fluid in the close vicinity of inner sphere has a lower density than that of near the outer sphere because the inner sphere is at higher temperature than that of outer sphere. Thus the fluid near the surface of the inner sphere moves downward. As the fluid moves downward, it loses energy and eventually forces the separation of the thermal boundary layer along the outer sphere. The heavy fluid then enters the thermal boundary of the inner sphere and completes the recirculation pattern. The centre of crescent shaped eddy stayed close to midgap but moved into the upper hemisphere as the Rayleigh number increases. This is apparent as we compare the radius ratio 2.2 in the Fig.4, where the Rayleigh number is $10^4$, with that in the Fig.5, where Ra=$10^5$. For the case of Ra= $10^5$ laminar convection is the more dominant of heat transfer than in Ra=$10^4$ As the circulation of fluid is more dominant in the upper zone making the outer layer warmer, while the lower domain is stagnant. The transport of the hot fluid to the outer layer is more prominent from the Fig. 4 and 5. For the conditions selected for fig.4 and 5 Pr=0.7 at different Ra value at rr value 2.2 the maximum values for stream function moves up ward as the Ra value increases. This behaviour can be shown from Fig 4 where for Ra=l$0^4$ $\psi_{max}$= 14.138164 obtains at angle =63°, while for Ra=l$0^5$ 28.772739 at angle =58.500004°.

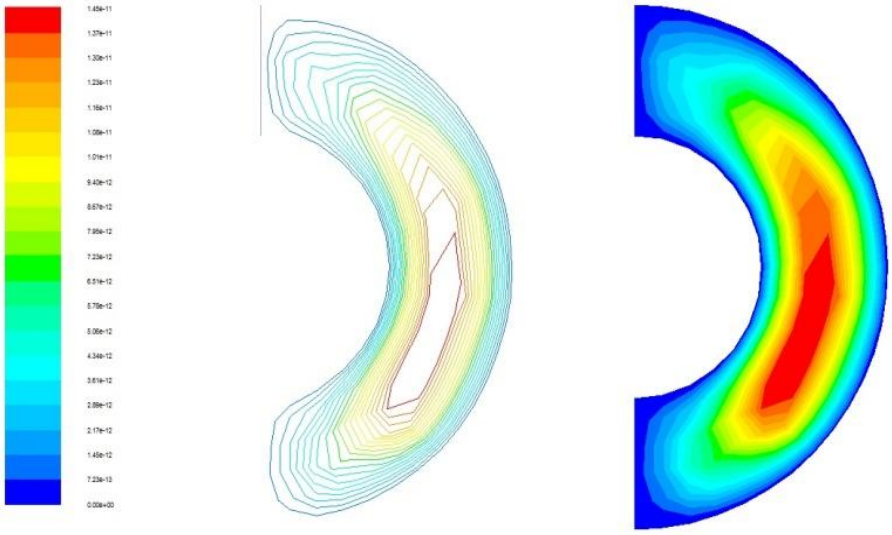

Figure 4 Isotherms and stream lines for Pr=0.7, rr = 2.0 at Ra= $10^4$ for Velocity distribution

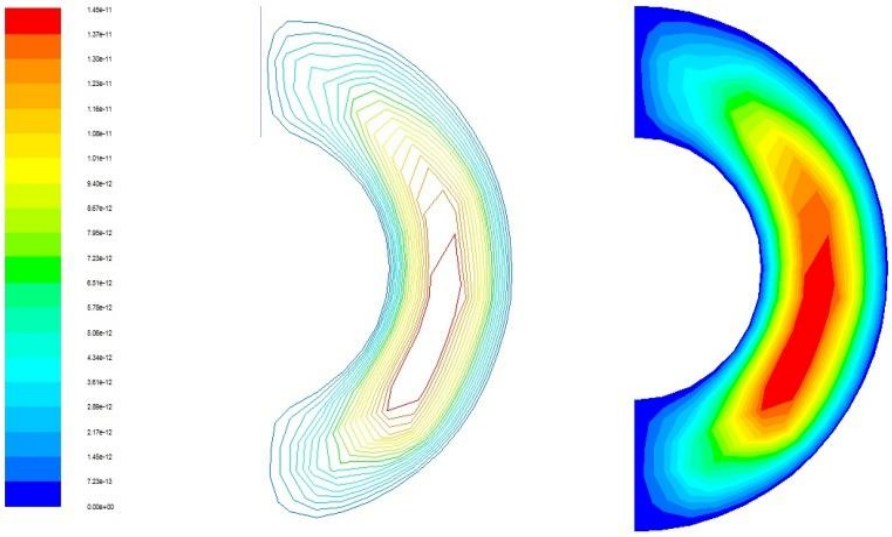

Figure 5 Isotherms and stream lines for Pr=0.7, rr = 2.2 at Ra= $10^5$ for Velocity distribution

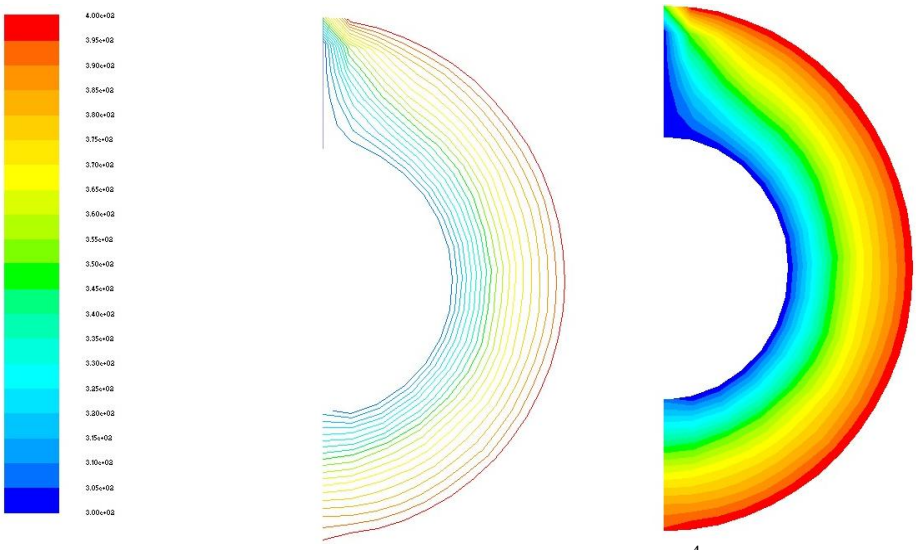

Figure 6 Isotherms and stream lines for Pr=0.7, rr = 2.2 at Ra= $10^4$ for Static temperature

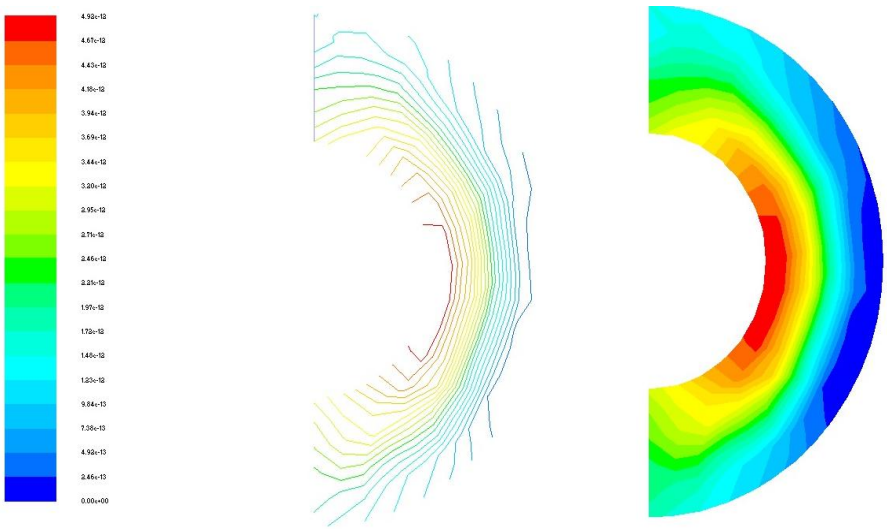

Figure 7 Counter of Stream Function of Spherical Annulus

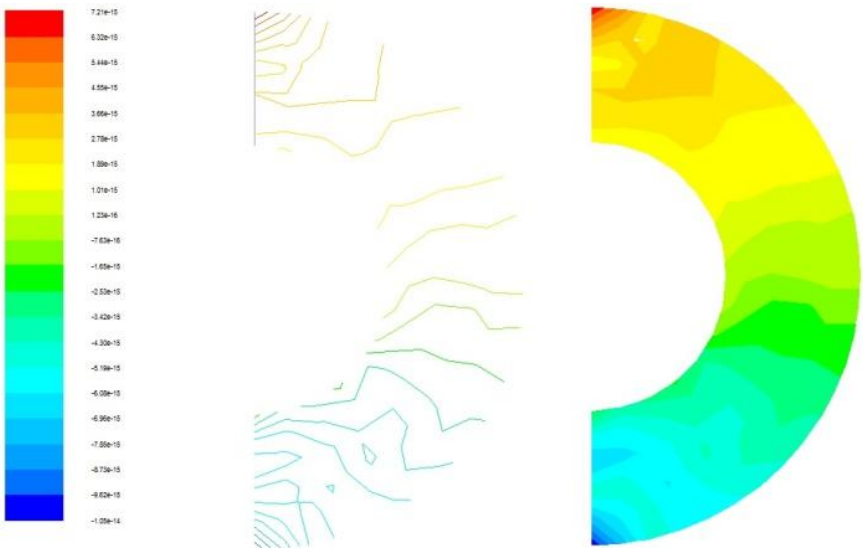

Figure 8 Isotherm and stream line contour of Static Pressure

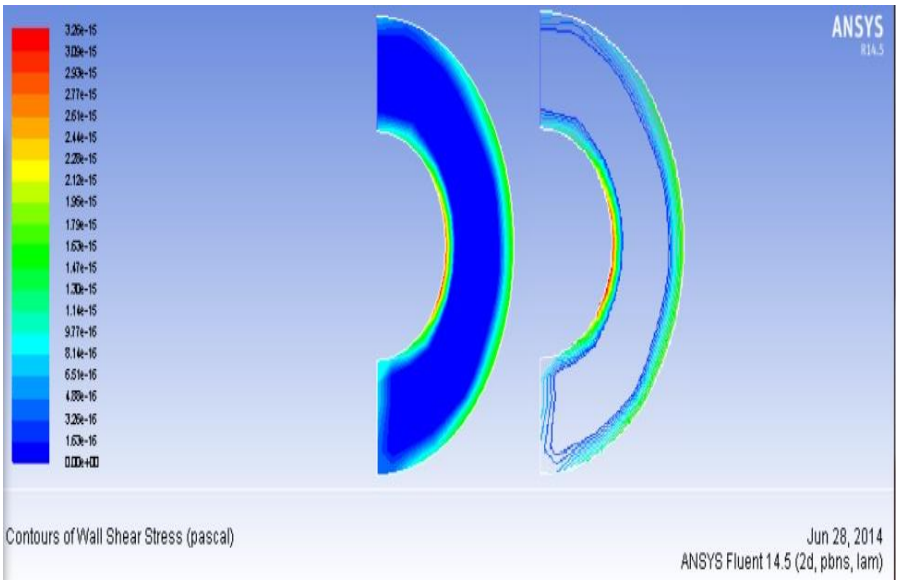


Figure 9 Isotherm and stream line contour of Wall shear stress

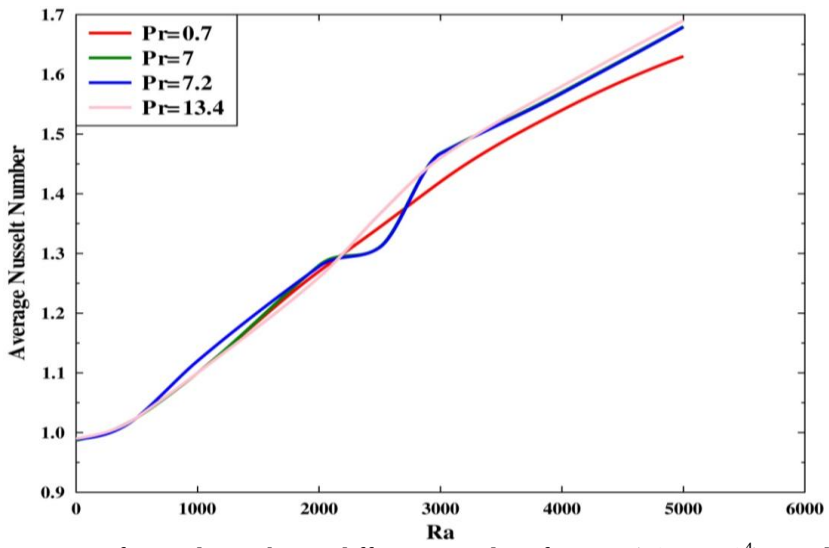


Figure 10 Variation of Nusselt number at different Pr values for Ra= (10 - $5x10^4$) at radius ratio 2.

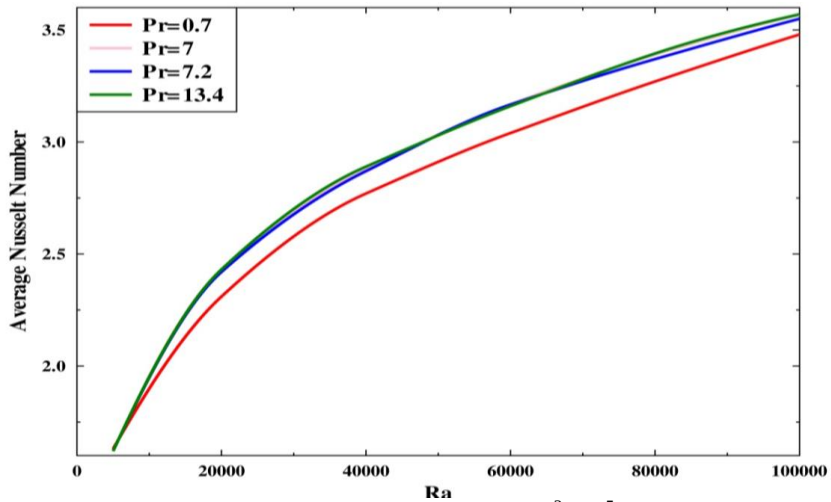


Figure 11 Variation of average Nu number and Ra. Number ($5x10^3$ -$10^5$) at different Prandlt No. for radius ratio 2

Figure 10 and 11 shows the variation of avg. Nusselt Numbers with Ra number at different Prandlt No. for radius ratio (rr = 2). Fig.10 shows the variations of avg. Nu. No where Ra. No. varies from $l0^1$-5x $10^3$.and in Fig 11 Ra. No. varies from $5xl0^3$-$10^5$. From the both the graphs two characteristics are being noticed; there is no effect or slight effect of Pr. No. on the heat transfer as the Rayleigh No increase. Another one, the Nusselt No varies almost linearly with Rayleigh No. As in the graphs the lines are nearly straight.

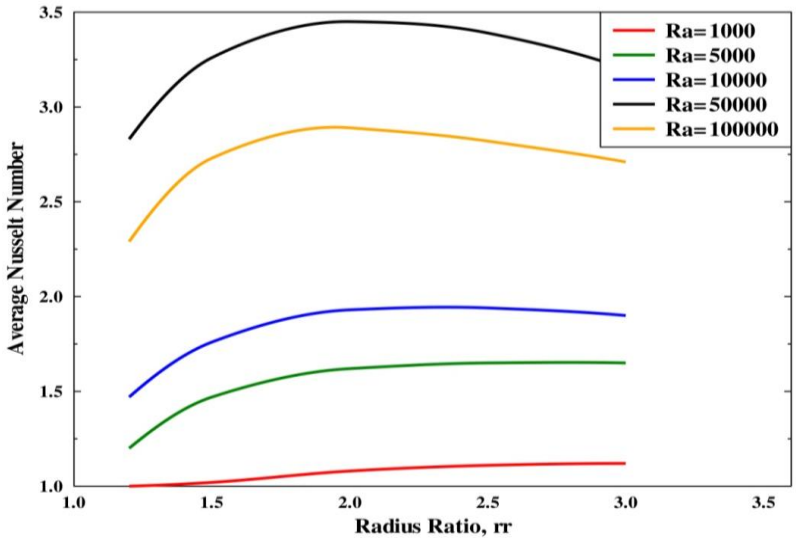


Figure 12 Variation of average Nusse1tnumber and Radius Ratio (rr) at different Rayeigh value.

Figure 12 shows the variation of avg. Nusselt No and the Radius Ratio at different Rayleigh No. Here we have taken Pr= 0.7 (for air) fixed. It has been seen that there is no influence of Prandlt values up on Nusselt number variation. It can also be conclude that for every Ra. value there is a critical radius ratio. Up to which the value of Nusselt No increases and after that it starts decreasing. The value of critical radius ratio decreases as the value of Rayleigh No. increases. Both the value of critical rr increases when Rayleigh No. varies up to 103.

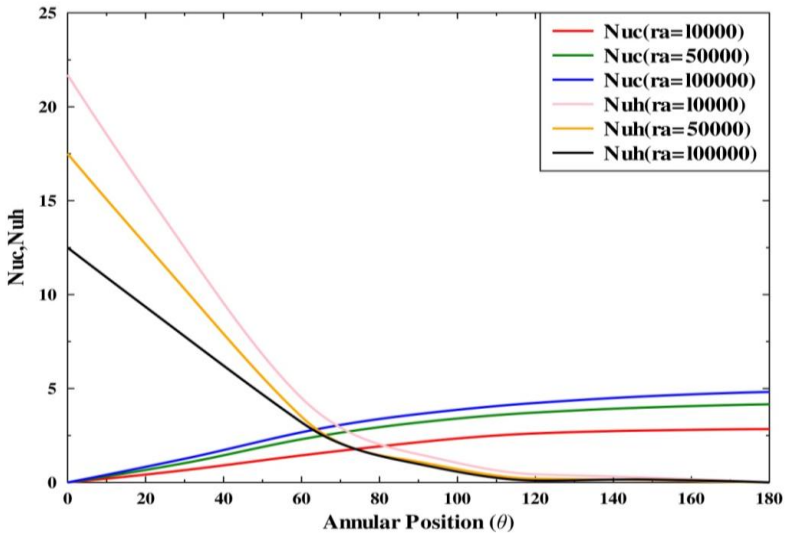


Figure 13 Steady local Nusselt number versus angular position at radius ratio 2 and Pr=0.7 at different Ra number

Fig.13 shows the distributions of steady local Nusselt numbers related to angular position when Rayleigh number changes, the effect of different Rayleigh number can be seen. According to the conditions Pr=0.7, rr =2, the local Nusselt number at the exterior of inner sphere have minimum value at a~o0.This implies that at upper symmetry the inner sphere has conduction and as the angular position increases natural convection becomes more dominant. While on the contrary at $\theta=0^0$ the portion near the outer sphere has convection as dominant mode for heat transfer and as the angular value increases the mode of heat transfer

changes towards conduction. The value of Nuh increases, the maximums occurs at θ=180°. The local Nusselt numbers on interior of outer sphere (Nuc) decreases gradually as angular position increases. The minimums are occurred at θ=180°. The whole variation is larger than Nuh. Nuc, decreases because the heat boundary layer becomes thicker as it moves downward and generates stagnation area at the bottom of outer sphere. Therefore the Nu, have big variation with angular positions as shown in fig.13.

## IV. CONCLUSION

The present work investigates computational the natural convection heat transfer of an Newtonian fluid contained between two concentric isothermal spheres. The behaviour of flow field and temperature field are shown graphically. The present results of local and average Nusselt number are in good agreement with the earlier works. The major results may be summarized below as follows:

- At fixed radius ratio the average Nusselt number increase with increase in Rayleigh number.
- At fixed Rayleigh number the Nusselt number first increases with increase in radius ratio, but after a critical radius ratio value Nusselt number stars decreasing.
- The centre of main vortex, where stream function is maximum, moves upward with increase in both Rayleigh number and radius ratio.
- Prandlt number has very slight effect upon Nusselt number if radius ratio has kept constant.

.

## REFERENCES


[1] L. R. Mack and H. C. Hardee, "Natural convection between concentric spheres at Low Rayleigh numbers", Int. J. Heat Mass Transfer 11, 387-396 (1968).

[2] S.H. Yin, R.E. Powe, J.A. Scanlan, E.H. Bishop, "Natural convection flow patterns in spherical annuli", International Journal of Heat and Mass Transfer, Volume 16, Issue 9, September 1973, Pages 1785-1786,IN1-IN4,1787-1795

[3] Ralph E. Powe, Jack A. Scanlan, Thomas A. Larson, "Flow studies for natural convection in liquids between a sphere and its cubical enclosure", International Journal of Heat and Mass Transfer, Volume 20, Issue 2, February 1977, Pages 159-169

[4] S. Ramadhyani, M. Zenouzi and K. N. Astill, "Combined Natural and Forced Convective Heat Transfer In Spherical Annuli", J. Heat Transfer 106(4), 811-816 (Nov 01, 1984) (6 pages) doi:10.1115/1.3246756History: Received April 29, 1984; Online October 20, 2009

[5] Sanjay K. Roy, Subrata Sengupta, "A numerical study of natural convection heat transfer in a vertically eccentric spherical annulus", International Communications in Heat and Mass Transfer, Volume 15, Issue 5, September–October 1988, Pages 615-626

[6] Vijay K. Garg, "Natural convection between concentric spheres", International Journal of Heat and Mass Transfer, Volume 35, Issue 8, August 1992, Pages 1935-1945

[7] Hsin-Sen Chu and Tzong-Shing Lee, "Transient natural convection heats transfer between Concentric spheres", Int.J. Heat and Mass transfer vol.36 N o. 13, pp.3159-3170(1993)

[8] C. P. Chiu, J. Y. Shich, and W. R. Chen, Tainan, Taiwan, "Transient natural convection of micropolar fluids in concentric spherical annuli", Acta Mechanica 132, 75-92 (1999)

[9] Vadim V. Travnikov, Hans J. Rath, Christoph Egbers "Stability of natural convection between spherical shells: energy theory", International Journal of Heat and Mass Transfer, Volume 45, Issue 20, September 2002, Pages 4227-4235

[10] Horng Wen Wu, Wen Ching Tsai, Huann-Ming Chou, "Transient natural convection heat transfer of fluids with variable viscosity between concentric and vertically eccentric spheres" International Journal of Heat and Mass Transfer, Volume 47, Issues 8–9, April 2004, Pages 1685-1700

[11] Wen Ruey Chen Æ Yen Hsun Chen, "Thermal effects of the micropolar fluid parameters on the laminar free convection in spherical annuli with mixed boundary conditions", Heat Mass Transfer (2008) 44:343–354

[12] Wen Ruey Chen, "Natural convection heat transfer between inner sphere and outer vertically eccentric cylinder", International Journal of Heat and Mass Transfer, Volume 53, Issues 23–24, November 2010, Pages 5147-5155

[13] R.S. Alassar ,"Conduction in eccentric spherical annuli", International Journal of Heat and Mass Transfer, Volume 54, Issues 15–16, July 2011, Pages 3796-3800

[14] Sangita, M. K. Sinha, R. V. Sharma, "Natural Convection in a Spherical Porous Annulus: The Brinkman Extended Darcy Flow Model", Transp Porous Med (2013) 100:321–335

[15] M. Hatami, GH.R. Mehdizadeh Ahangar, D.D. Ganji, K. Boubaker "Refrigeration efficiency analysis for fully wet semi-spherical porous fins", Energy Conversion and Management, Volume 84, August 2014, Pages 533-540}J. M. Burgess, "Fuel Combustion in the Blast Furnace Raceway Zone", Pro 9. Energy Combust. Sci. 1985, Vol. 11, pp. 61 82

**Nomenclature**

| | |
|---|---|
| g | acceleration due to gravity thermal diffusivity of the fluid.[m/s$^2$] |
| k | Thermal conductivity of the fluid the fluid,[W/m-k] |
| Pr | Prandtl number of the fluid |
| $r_i$, $r_o$ | Radii of inner and outer spheres respectively, [m] |
| d | thickness,[m] |
| rr | Radius Ratio |
| R | Dimensionless radial coordinate |
| θ | Dimensionless angular coordinate |
| Ra | Rayleigh number based |
| Gr | Grashof number |
| T | Temperature of the fluid [K] |
| Ti, To | Temperature of the inner and outer spheres, respectively[K] |
| u | velocity component in the r- direction.[rn/s$^2$] |
| U | dimensionless velocity component r- direction |
| v | velocity component in 8 -direction,[m/s$^2$] |
| V | dimensionless velocity component in in 8 –direction |
| $Nu_h$ | Average Nusselt Number on hot sphere |
| $Nu_c$ | Average Nusselt number on cold sphere |
| ΔR | Small interval in R-direction |
| Δθ | Small interval in B direction |

**Greek Symbols**

| | |
|---|---|
| α | Thermal diffusivity of the fluid |
| β | Coefficient of volumetric expansion |
| μ | Kinematic viscosity |
| ρ | Density of fluid |
| ρm | Density of fluid at Tm |
| ΔR | Mesh size in the radial direction |
| Δθ | Mesh size in the B –direction |
| T | Dimensionless temperature |
| Y | Kinematic viscosity of the fluid |
| Ψ | Stream function |
| Ω | Vorticity |